Probing Outer-Sphere Adsorption of Aqueous Metal Complexes at the Oxide-Water Interface with Resonant Anomalous X-Ray Reflectivity

Changyong Park,[1] Paul A. Fenter,[1] Neil C. Sturchio,[1,2] and John R. Regalbuto[3]

[1]*Environmental Research Division, Argonne National Laboratory, Argonne, Illinois 60439, USA*

[2]*Department of Earth and Environmental Sciences, University of Illinois at Chicago, Chicago, Illinois 60607, USA*

[3]*Department of Chemical Engineering, University of Illinois at Chicago, Chicago, Illinois 60607, USA*

(Received 10 September 2004; published 25 February 2005)

Resonant anomalous x-ray reflectivity near the Pt L_{III} edge simultaneously revealed the geometric and spectroscopic structures of $Pt(NH_3)_4^{2+}$ ions adsorbed at the quartz(100)-water interface. The derived Pt geometric subprofile shows two discrete ''outer-sphere'' adsorbed layers, and the interface-specific x-ray absorption edge profile exhibits a significant white-line enhancement compared to the bulk-solution species.

DOI: 10.1103/PhysRevLett.94.076104 PACS numbers: 68.08.De, 61.10.Eq, 68.43.Fg, 82.65.+r

Interactions of metal oxide surfaces with aqueous metal ions control a wide range of reaction and transport processes in natural systems and industrial applications, such as ore processing, water treatment, corrosion inhibition, and catalyst preparation. A key distinction in the nature of aqueous-ion-oxide interactions is whether the ion's hydration sphere is disrupted allowing it to form strong chemical bonds with oxygen atoms of the substrate (i.e., inner-sphere surface complex), or if the ion retains its hydration sphere so that there can be one or more intervening water layers between it and the substrate (either as a discrete outer-sphere surface complex [1] or a continuous Gouy-Chapman diffuse ion distribution [2]). Conventional spectroscopic approaches for characterizing such interfacial systems *in situ* (e.g., x-ray fluorescence) are not inherently interface specific, and therefore interfacial signals can be obscured by fluorescence from solution species. Such limitations can be effectively bypassed by combining surface-specific resonant anomalous x-ray reflectivity (RAXR; elastic scattering intensity vs incident photon energy) [3] with conventional surface x-ray reflectivity (scattering intensity vs momentum transfer), simultaneously exploiting both element-specific anomalous x-ray dispersion near an x-ray absorption edge and the surface sensitivity of x-ray reflectivity. RAXR has been applied previously to studies of film-substrate registry [4–6], hetero-structure interface [7], and the oxidation state of buried interfaces or electrode metal surfaces [8,9], where either the geometric or spectroscopic structure was known *a priori*. Here we report the ability of RAXR to yield simultaneous interface-specific geometric and spectroscopic adsorbate structures of weakly adsorbed surface complexes at the mineral-water interface.

In this Letter we explore the physical structure and spectroscopic properties of platinum tetraammine [PTA; $Pt(NH_3)_4^{2+}$] adsorbed at the quartz(100)-water interface. This system represents the initial step in noble metal catalyst impregnation and is a good analogue for many natural adsorption processes. The goals of noble metal catalyst impregnation are high surface coverage, small metal particles, and efficient metal use via high active surface area. These goals are normally assumed to require strong metal precursor-oxide interaction [10]. Quantitative modeling of such interfacial systems is relatively new; the earliest efforts employed parameter-laden triple-layer models [11,12] and assumed inner-sphere adsorption of the precursor at the oxide-water interface. However, recent reports suggest that the interaction of ionic Pt complexes with common catalyst support oxides is purely electrostatic [13,14], possibly implying outer-sphere complexes or a diffuse ion distribution. These differences can be directly distinguished through the use of an *in situ* probe of the interfacial structure.

PTA is readily adsorbed to the negatively charged quartz surface from dilute (~200 ppm) $Pt(NH_3)_4Cl_2$ solutions at

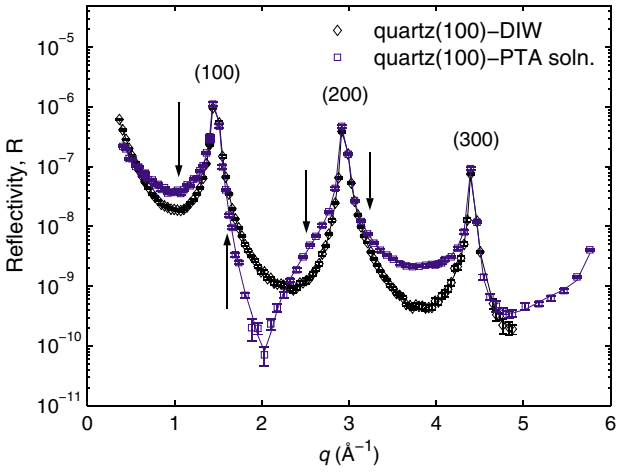

FIG. 1 (color). Specular x-ray reflectivity vs momentum transfer for the quartz (100) surface in contact with deionized water and 200-ppm PTA at pH ~ 10. Calculations (solid lines) are derived from nonlinear least-squares fits to the data. The vertical arrows indicate the selected q positions at which the RAXR spectra were measured.

pH ~ 10 [13]. The quartz (100) surface was chosen because its geometric structure in contact with water is known [15], and its surface functional groups (terminal silanol groups and bridging oxygens) are similar to those of the amorphous silica used as a catalyst support. High-resolution nonresonant specular x-ray reflectivity data for the single-crystal quartz(100)-water interface with and without PTA are shown in Fig. 1 as a function of momentum transfer, $q = 4\pi \sin(\alpha)/\lambda$ (where α is the incident angle of x-ray photons), at fixed energy ($E = 20$ keV). RAXR spectra of adsorbed PTA (Fig. 2) were measured near the Pt L_{III} edge (11.564 keV) at fixed momentum transfer values ($q_0 = 1.03$, 1.62, 2.50, and 3.24 Å^{-1}) indicated by arrows in Fig. 1. Measurements were made at beam line 12-BM-B [16] (BESSRC-CAT) at the Advanced Photon Source (for details of sample preparation and procedures, see Refs. [17,18]).

The nonresonant reflectivity $R(q)$ of a solid-liquid interfacial system is proportional to the squared magnitude of the total nonresonant structure factor $F_{\mathrm{NR}}(q)$, which is related to the laterally averaged total electron density $\rho(z)$ by

$$R(q) \propto |F_{\mathrm{NR}}(q)|^2 = \left| \int \rho(z) \exp(iqz) dz \right|^2 = \left| \sum_k^{\infty} \theta_k f_k(q) \exp(iqz_k) \exp(-q^2\sigma_k^2/2) \right|^2. \quad (1)$$

Here, θ_k is the occupancy, $f_k(q)$ is the atomic form factor, and σ_k is the root mean square width of a Gaussian distribution of the kth atom in the system. In Fig. 1, sensitivity of the nonresonant data to the interfacial structure is seen in large changes in specular intensity upon PTA adsorption. The interfacial structure [blue line in Fig. 3(a)], and consequently $F_{\mathrm{NR}}(q)$ in Eq. (1), was obtained in the context of a "water-equivalent profile," by assuming that all contributions above the quartz surface derive from water and is compared to the initial quartz(100)-water interface structure (black line). In spite

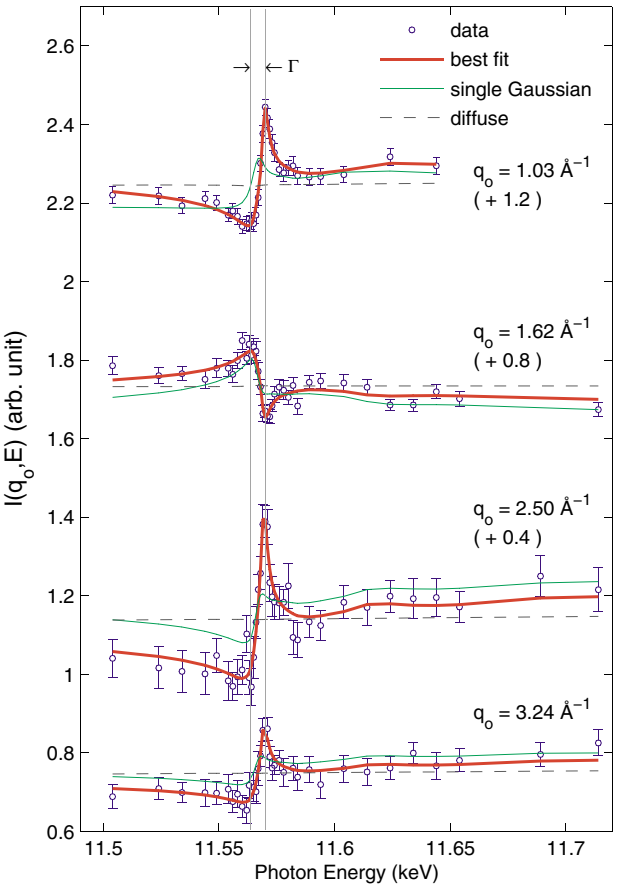

FIG. 2 (color). RAXR spectra normalized with nonresonant reflectivity near the Pt L_{III} edge (11.564 keV) of the quartz(100)-PTA interface at selected momentum transfers. Lines represent calculations corresponding to the best-fit model (red thick lines) and two other models described in the text. The vertical lines indicate the energies noted in Fig. 3(b). Data are offset vertically as indicated for clarification.

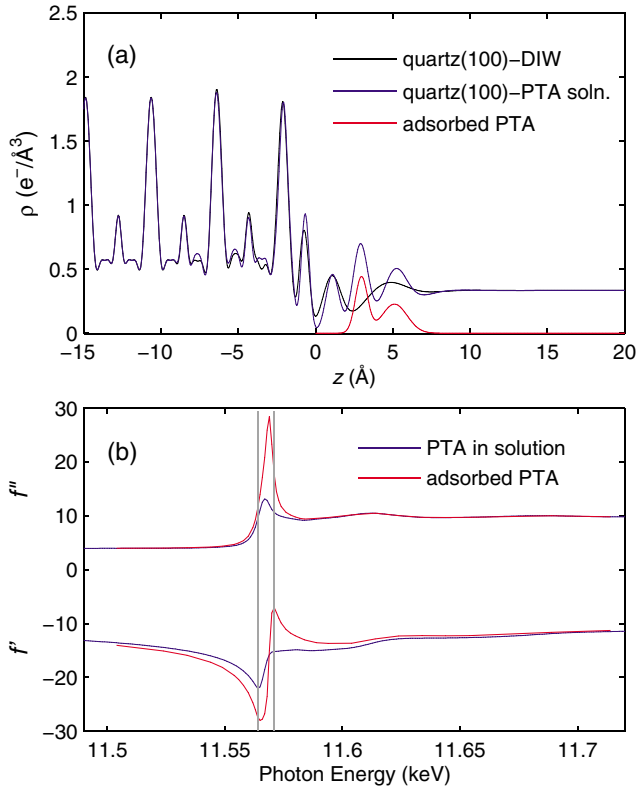

FIG. 3 (color). (a) Derived resolution-broadened interfacial profiles [18] of quartz (100) surfaces in contact with deionized water and 200-ppm PTA at pH ~ 10. The Pt-specific profile of adsorbed PTA is also shown. The peaks at $z < 0$ Å correspond to quartz lattice atoms, and the peak at $z \sim 1$ Å corresponds to "adsorbed" water. (b) Derived $f_{\mathrm{Pt}}'(E)$ and $f_{\mathrm{Pt}}''(E)$ of PTA. The vertical lines represent the positions of the minimum and the maximum of $f_{\mathrm{Pt}}'(E)$ near the Pt L_{III} edge (at 11.564 and 11.570 keV, respectively) for the adsorbed PTA species. The relative difference of 6 eV corresponds to the width of the white-line (Γ) in $f_{\mathrm{Pt}}''(E)$ for the adsorbed Pt species.

of large changes in the data, changes in the interfacial structure are relatively small, and the PTA location cannot be uniquely associated with any individual peaks in the electron density profile. For example, analysis of the nonresonant data in Fig. 1 after assignment of Pt to one or more of the interfacial layers results in indistinguishable qualities of fit and derived density profiles.

The RAXR spectra (Fig. 2) can be used to directly probe the Pt-specific structure. These spectra are derived solely from elastic scattering and thus are related only to the coherently adsorbed interfacial species. The scattering intensity is modulated as a function of incident photon energy by anomalous dispersion of the resonant atomic scattering factor $f(q_0, E) = f_{\mathrm{NR}}{}^0(q_0) + f_{\mathrm{R}}{}'(E) + if_{\mathrm{R}}{}''(E)$, where $f_{\mathrm{NR}}{}^0(q_0)$ corresponds to the nonresonant scattering factor as used in Eq. (1), and $f_{\mathrm{R}}{}'(E)$ and $f_{\mathrm{R}}{}''(E)$ are related by Kramers-Kronig dispersion relationships [19]. The resonant total structure factor at a fixed momentum transfer q_0 can be expressed as $F(q_0, E) = F_{\mathrm{NR}}(q_0) + F_{\mathrm{R}}(q_0, E)$ where,

$$F_{\mathrm{R}}(q_0, E) = \sum_j \theta_j [f_j'(E) + if_j''(E)] \exp(iq_0 z_j) \times \exp(-q_0^2 \sigma_j^2/2). \quad (2)$$

Here, $F_{\mathrm{NR}}(q_0)$ and $F_{\mathrm{R}}(q_0, E)$ correspond to the nonresonant and resonant parts of the structure factor, and the sum is over j resonant components. The q-dependent atomic scattering factor of the resonant atom, $f_j^0(q_0)$, is included in $F_{\mathrm{NR}}(q_0)$ in Eq. (2) as a water-equivalent component, and the q dependence of anomalous dispersion, $f_{\mathrm{R}}{}' + if_{\mathrm{R}}{}''$, is negligible [19]. Equation (2) suggests a new approach for understanding the RAXR data in Fig. 2: with the total nonresonant structure factor determined independently by the derived total density profile in Fig. 3(a), the RAXR data are constrained by the resonant atom's geometric (θ_j, z_j, σ_j) and spectroscopic (f_j', f_j'') structures.

Direct insight into the data of Fig. 2 can be obtained by normalizing Eq. (2) to the nonresonant reflectivity:

$$\left| \frac{F(q_0, E)}{F_{\mathrm{NR}}(q_0)} \right|^2 = 1 + \left| \frac{F_{\mathrm{R}}(q_0, E)}{F_{\mathrm{NR}}(q_0)} \right|^2 + 2 \left| \frac{F_{\mathrm{R}}(q_0, E)}{F_{\mathrm{NR}}(q_0)} \right| \times \cos[\phi_{\mathrm{NR}}(q_0) - \phi_{\mathrm{R}}(q_0, E)]. \quad (3)$$

Here, $\phi_{\mathrm{NR}}(q_0)$ and $\phi_{\mathrm{R}}(q_0, E)$ represent the phases of the nonresonant and resonant structure factors, respectively. This expression shows that the changes in the normalized resonant intensities are usually large where the nonresonant reflectivity signal is small. The resonant modulation should also change in sign whenever the cosine term equals to zero, as seen in the experimental data when comparing spectra at $q_0 = 1.03$, 1.62, and again at 2.5 Å^{-1}.

Direct information concerning the average Pt height comes through examination of this behavior at small q and for $E < E_{\mathrm{Pt}\,L_{\mathrm{III}}}$, where $f'(E)$ is increasingly negative and $f''(E)$ is small and approximately constant. Choosing the mathematical origin at the unit cell border [as shown in Fig. 3(a)] so that $\phi_{\mathrm{NR}}(q) \approx -\pi/2$ below the first Bragg peak, we see that the phase inversion takes place whenever $\phi_{\mathrm{R}} = n\pi$ ($n =$ integer). Also, since the phase due to anomalous dispersion of the Pt form factor is small (i.e., $\mathrm{atan}[f_{\mathrm{Pt}}{}''(E)/f_{\mathrm{Pt}}{}'(E)] \ll \pi$), we find that $\phi_{\mathrm{R}}(q, E) \approx q\langle z \rangle$, where $\langle z \rangle$ is the average height of the Pt distribution. Consequently, the first phase inversion takes place at $q \approx \pi/\langle z \rangle$, and the resonant intensity should show a *positive* slope for $E < E_{\mathrm{Pt}\,L_{\mathrm{III}}}$ when the phase associated with the resonating atom's height, $q\langle z \rangle$, is small. The data show that RAXR intensity has a *negative* slope for $E < E_{\mathrm{Pt}\,L_{\mathrm{III}}}$ at $q_0 = 1.03$ Å^{-1} (Fig. 2), which suggests that the phase term in Eq. (3) has already changed in sign below $q_0 = 1.03$ Å^{-1}, and consequently the average Pt height is >3 Å above the origin in Fig. 3(a). Because the average PTA height is significantly above the surface hydration layer locating at $z \sim 1$ Å, this immediately suggests an "outer-sphere" or "diffuse ion distribution" mode for PTA adsorption.

Calculated RAXR spectra for an exponentially decaying diffuse ion distribution with an expected Debye length of 56 Å derived from the Gouy-Chapman model results in negligible modulation in the RAXR spectra for each q_0 that was measured (black dashed lines, Fig. 2). This, coupled with the significant modulation observed even at 3.24 Å^{-1}, leads to the conclusion that the Pt distribution is primarily in the form of an adsorbed species with a narrow height distribution. A single Gaussian distribution with bulk-solution XANES profiles [blue solid lines in Fig. 3(b)] [20] leads to a derived height of ~3.0 Å, roughly consistent with the model independent analysis above, but the quality of fit is poor ($\chi^2 = 4.6$) and many qualitative features of the RAXR data are not properly explained (thin green lines, Fig. 2). These RAXR data therefore strongly suggest that the geometric and/or spectroscopic structures of the actual PTA species are more complex than anticipated.

Analysis of the RAXR data through nonlinear least-squares fits to model structures (thick red lines in Fig. 2) results in satisfactory agreement only when the Pt distribution contains at least two distinct layers [Fig. 3(a), red solid line] and the interface-specific anomalous dispersion (i.e., the XANES profile) contains a substantial white-line enhancement at the Pt L_{III} edge [Fig. 3(b), red solid lines]. The best-fit geometric structure is described by the parameters $\theta_1 = 0.15 \pm 0.02$ ML, $z_1 = 2.97 \pm 0.02$ Å, and $\sigma_1 = 0.20 \pm 0.06$ Å for the first layer and $\theta_2 = 0.16 \pm 0.03$ ML, $z_2 = 5.11 \pm 0.05$ Å, and $\sigma_2 = 0.74 \pm 0.07$ Å for the second layer (1 ML ≡ 1Pt/26.566 Å^2). The nontrivial agreement between the derived Pt substructure and similar features in the total electron density plot [Fig. 3(a)], both in size and location, is direct evidence of the consistency of the nonresonant and resonant structural analyses. This result clearly shows that the Pt distribution is in the

form of an ''outer-sphere'' adsorbate [1], because PTA is not incorporated into the surface hydration layer at $z \sim 1$ Å [Fig. 3(a)], as would be characteristic of ''inner-sphere'' adsorbates [21]. The derived f_{Pt}'' and f_{Pt}' spectra for the adsorbed species [red solid lines in Fig. 3(b)] are obtained by adding a Lorentzian white-line (height 16.5 ± 3 eu, width 3.6 ± 0.4 eV, center 11568.9 ± 0.15 eV) and its Kramers-Kronig counterpart [22] to the solution's PTA anomalous dispersion spectra [blue solid lines in Fig. 3(b)] [20], obtained by using the difference Kramers-Kronig transform technique [23]. These spectra show substantial white-line enhancement relative to the solution XANES for both adsorbed PTA species.

A geometric model consistent with these observations suggests that the large hydrated, square planar PTA complex adsorbs by ''lying down,'' presumably so that Pt can be coordinated with the surface hydration layer and simultaneously maximize electrostatic energy between PTA and the charged surface sites. Here the white-line enhancement may be due to polarization-dependent transition probabilities, as shown in Ref. [24]. Other mechanisms to explain this white-line enhancement involve structural or chemical modification of the adsorbed PTA species. For instance, the derived spectrum is comparable to those of α-PtO_2 and $Na_2Pt(OH)_6$ [25], possibly indicating that the adsorbed Pt complex is octahedrally coordinated and oxidized with respect to the solution PTA species (e.g., due to the x-ray beam [26]). This is inconsistent with the known electrostatically controlled adsorption, because oxidized Pt species are anionic and should be repelled from the negatively charged quartz surface [13]. Also, the incident beam flux was sufficiently small that negligible oxidation should have taken place under our experimental conditions. Full resolution of these issues may require improved understanding of polarization-dependent transition probabilities.

These results demonstrate a useful element-specific approach for probing ion adsorption at the oxide-water interface and show that adsorption of electrostatically bound aqueous metal complexes at the oxide-water interface can exhibit complexities that can be understood only when both the geometric and spectroscopic substructures are fully resolved. This behavior highlights the need for a deeper understanding of such systems, especially in regard to the central role of ion-oxide interactions at the liquid-solid interface in technology (e.g., noble metal catalyst preparation) and nature (e.g., transport of nutrients and pollutants in the environment).

This work was supported by the Geosciences Research Program of the Office of Basic Energy Sciences, U.S. Department of Energy, through Contract No. W-31-109-ENG-38 to Argonne National Laboratory, and by National Science Foundation Grant No. CTS-0243210 (J. R. R.). Measurements were made at beam lines 12-BM-B and 11-ID-D of the Basic Energy Sciences Synchrotron Radiation Center, Advanced Photon Source. We thank A. J. Kropf and J. T. Miller for unpublished PTA XANES spectra.

[1] K. F. Hayes *et al.*, Science **238**, 783 (1987).
[2] M. J. Bedzyk *et al.*, Science **248**, 52 (1990).
[3] F. J. Walker and E. D. Specht, in *Resonant Anomalous X-ray Scattering: Theory and Applications*, edited by G. Materlik, C. J. Sparks, and K. Fischer, (Elsevier Science, Amsterdam, 1994), pp. 365–387.
[4] K. Akimoto, K. Hirose, and J. Mizuki, Phys. Rev. B **44**, 1622 (1991).
[5] F. J. Walker, E. D. Specht, and R. A. Mckee, Phys. Rev. Lett. **67**, 2818 (1991).
[6] I. M. Tidswell *et al.*, Phys. Rev. B **51**, 10205 (1995).
[7] I. K. Robinson *et al.*, Appl. Phys. Lett. **79**, 2913 (2001).
[8] E. D. Specht and F. J. Walker, Phys. Rev. B **47**, 13743 (1993).
[9] Y. S. Chu *et al.*, Phys. Rev. Lett. **83**, 552 (1999).
[10] J. P. Brunelle, Pure & Appl. Chem. **50**, 1211 (1978).
[11] T. Mang *et al.*, Appl. Catal., A **106**, 239 (1993).
[12] K. Bourikas *et al.*, J. Phys. Chem. **100**, 11711 (1996).
[13] M. Schreier and J. R. Regalbuto, J. Catal. **225**, 190 (2004).
[14] X. Hao, W. A. Spieker, and J. R. Regalbuto, J. Colloid Interface Sci. **267**, 259 (2003).
[15] M. L. Schlegel *et al.*, Geochim. Cosmochim. Acta **66**, 3037 (2002).
[16] M. A. Beno *et al.*, Nucl. Instrum. Methods Phys. Res., Sect. A **467**, 699 (2001).
[17] The quartz (100) natural growth surface sample was prepared as described previously [15]. The sample crystal was mounted in a thin film cell in deionized water for alignment, and PTA adsorption and equilibration was obtained by repeatedly flushing 200 ppm PTA *p*H 10 solutions so that the hydrated $Pt(NH_4)^{2+}$ complexes are adsorbed at a negatively charged quartz (100) surface. Reversibility of adsorption and *p*H control were confirmed by desorption of the Pt species upon exposure to a 1*M* NaCl solution at *p*H $\sim$ 3. The x-ray reflectivity was distinguished from background signals (including Pt fluorescence) with rocking scans at each momentum transfer. Derived structures and estimated uncertainties are obtained by least-squares optimization of atomistic structural models as described previously [18].
[18] P. A. Fenter, in *Reviews in Mineralogy and Geochemistry*, edited by P. A. Fenter, M. L. Rivers, N. C. Sturchio, and S. R. Sutton (Mineralogical Society of America, Washington, 2002), Vol. 49, pp. 149–220.
[19] J. Als-Nielsen and D. McMorrow, *Elements of Modern X-ray Physics* (Wiley, New York, 2001).
[20] $f_{Pt}''(E)$ of the PTA solution species were derived from measured XANES spectra of 1000 ppm PTA in NH_4OH solution, courtesy of A. J. Kropf, Argonne National Laboratory.
[21] Z. Zhang *et al.*, Surf. Sci. **554**, L95 (2004).
[22] K. Ohta and H. Ishida, Appl. Spectrosc. **42**, 952 (1988).
[23] J. O. Cross *et al.*, Phys. Rev. B **58**, 11215 (1998).
[24] D. H. Templeton and L. K. Templeton, Acta Crystallogr. Sect. A **41**, 365 (1985).
[25] A. N. Mansour *et al.*, J. Phys. Chem. **88**, 1778 (1984).
[26] J. T. Miller, private communication (unpublished data).